Quantification of the Tropospheric Removal of Chloral (CCl_3CHO): Rate Coefficient for the Reaction with OH, UV Absorption Cross Sections, and Quantum Yields

Ranajit K. Talukdar,*,†,‡ Abdelwahid Mellouki,§ James B. Burkholder,† Mary K. Gilles,†,‡ Georges Le Bras,§ and A. R. Ravishankara†,‡,||

Aeronomy Laboratory, National Oceanic and Atmospheric Administration, 325 Broadway, R/AL2, Boulder, Colorado 80305-3338, Cooperative Institute for Research in Environmental Sciences, University of Colorado, Boulder, Colorado 80309, and CNRS-LCSR, 45071 Orléans, Cedex 02-France

Received: December 31, 2000; In Final Form: March 15, 2001

Rate coefficients for the reaction, OH + CCl_3CHO (chloral) → products (k_5), were measured over the temperature range 233−415 K using the pulsed laser photolysis-laser-induced fluorescence method, and were determined to be $k_5(T) = (1.79 \pm 0.17) \times 10^{-12} \exp[-(240 \pm 60)/T]$ cm^3 molecule^{-1} s^{-1}. The quoted uncertainties are at the 95% confidence level with $\sigma_A = A\sigma_{\ln A}$, and include estimated systematic errors. Our results are compared with those from previous work and the differences are discussed. UV absorption cross sections of CCl_3CHO were measured between 200 and 345 nm and over the temperature range 240−360 K. These measurements are in good agreement with previously reported values. The quantum yields for O, H, and Cl atoms in CCl_3CHO photolysis were measured via atomic resonance fluorescence detection following pulsed excimer photolysis. Upper limits for the O atom quantum yield in CCl_3CHO photolysis at 308 and 248 nm were measured to be <0.01 and <0.02, respectively. The H atom quantum yields in CCl_3CHO photolysis at 193, 248, and 308 nm were 0.04 ± 0.01, <0.01, and <0.002, respectively. The Cl atom quantum yield in the photolysis of CCl_3CHO at 308 nm was 1.3 ± 0.3. The rate coefficient for the reaction Cl + CCl_3CHO was determined to be $k_8(298\text{ K}) = (5.4 \pm 0.7) \times 10^{-12}$ cm^3 molecule^{-1} s^{-1}. These results are used to evaluate the tropospheric lifetime of CCl_3CHO and the significance of chlorine transport from methylchloroform degradation to the lower stratosphere.

Introduction

Chloral (CCl_3CHO) can be a stable product in the atmospheric degradation of organic compounds containing more than two carbons and a CCl_3 group. There are no significant anthropogenic sources of CCl_3CHO and methylchloroform (CH_3CCl_3) is the primary source of CCl_3CHO in the atmosphere. Chloral is produced from CH_3CCl_3 via the following reaction sequence:

$$OH + CH_3CCl_3 \rightarrow H_2O + CCl_3CH_2 \quad (1)$$

$$CCl_3CH_2 + O_2 + M \rightarrow CCl_3C(OO)H_2 + M \quad (2)$$

$$CCl_3C(OO)H_2 + NO \rightarrow CCl_3C(O)H_2 + NO_2 \quad (3)$$

$$CCl_3C(O)H_2 + O_2 \rightarrow CCl_3CHO + HO_2 \quad (4)$$

In the determination of the ozone depletion potential of a compound such as CH_3CCl_3, it is necessary to understand not only its atmospheric lifetime but also those of its degradation products. Degradation products containing halogens produced in the troposphere may still transport halogen to the stratosphere. Therefore, in the case of methylchloroform, a complete evaluation of the impact of CH_3CCl_3 on the atmosphere needs an understanding of the atmospheric loss processes of CCl_3CHO, and its degradation products.

CCl_3CHO is expected to have a relatively short atmospheric lifetime due to its loss via reaction with the OH radical, UV photolysis, and dry and wet deposition.[1,2] The rate coefficient for the reaction of the OH radical with chloral,

$$OH + CCl_3CHO \rightarrow \text{products} \quad (5)$$

has been investigated previously.[1,3−6] However, there are considerable discrepancies among the reported values of k_5, which range from (8.6 to 18) × 10^{-13} cm^3 molecule^{-1} s^{-1}, at 298 K. To our knowledge, only one measurement of its temperature dependence, by Dóbé et al.[4] between 298 and 520 K, has been reported ($k_5(T) = (1.56 \pm 0.33) \times 10^{-12} \exp[-(600 \pm 100)/T]$ cm^3 molecule^{-1} s^{-1}). However, Dóbé et al. did not cover tropospheric temperatures (i.e., T <298 K). Therefore, further measurements of k_5 are warranted.

CCl_3CHO has a UV absorption spectrum typical of aldehydes and shows a strong absorption at wavelengths less than 250 nm and another weak electronic transition in the actinic region of the atmosphere, >290 nm. Photolysis of CCl_3CHO in the atmosphere will occur almost exclusively via this weak transition. The possible photolysis channels available in this wavelength region are

$$CCl_3CHO + h\nu \rightarrow CCl_3 + CHO$$
$$\Delta H_f^\circ(298\text{ K}) = 69 \text{ kcal mol}^{-1}, \lambda = 415 \text{ nm} \quad (6a)$$
$$\rightarrow CCl_3CO + H$$
$$\Delta H_f^\circ(298\text{ K}) = 87.5 \text{ kcal mol}^{-1}, \lambda = 327 \text{ nm} \quad (6b)$$
$$\rightarrow Cl + CCl_2CHO$$
$$\Delta H_f^\circ(298\text{ K}) = 71 \text{ kcal mol}^{-1}, \lambda = 403 \text{ nm} \quad (6c)$$
$$\rightarrow CCl_3H + CO$$
$$\Delta H_f^\circ(298\text{ K}) = -9 \text{ kcal mol}^{-1} \quad (6d)$$

The wavelengths listed with each photolysis channel are the

10.1021/jp004632j CCC: $20.00 © 2001 American Chemical Society
Published on Web 05/05/2001

energetic thresholds calculated using the thermochemical data from DeMore et al.,[7] Rayez et al.,[8] and the others noted below. The additivity method of Benson[9,10] was used for estimating the heat of formation of CCl_3CHO ($\Delta H_f°(298\ K) = -42.0$ kcal mol^{-1}). This value can also be estimated by taking the average of the heats of formation of C_2Cl_6 ($\Delta H_f°(298\ K) = -35.3$ kcal mol^{-1}) and $(CHO)_2$, glyoxal, ($\Delta H_f°(298\ K) = -48.5$ kcal mol^{-1}). The dissociation energy for (6c) is the average of the C−Cl bond dissociation energies in $Cl-CCl_3$, $Cl-CHCl_2$, and CF_2ClCCl_2-Cl. A full evaluation of the photolytic loss of chloral in the atmosphere requires accurate knowledge of its UV absorption cross sections as a function of temperature, the quantum yield for its photodissociation over the range of actinic wavelengths, and identification of the photoproducts.

The UV absorption cross sections of chloral have been reported by Gillotay et al.[11] and Rattigan et al.[2] at $T \leq 298$ K. Gillotay et al. reported absorption cross sections between 170 and 320 nm for temperatures ranging from 210 to 295 K, while Rattigan et al.[2] covered 200−360 nm at 296 and 243 K. However, there are significant differences between the two data sets in the wavelength range of atmospheric interest. To our knowledge, there are no quantitative measurements of the quantum yields for photodissociation of CCl_3CHO or for formation of products.

The Henry's law solubility constant of chloral (3.4×10^5 M atm^{-1})[12] is the only available information on its possible wet chemistry. There are no other data for the evaluation of the heterogeneous loss of chloral in the atmosphere.

In this paper, we report rate coefficients for reaction 5, k_5, between 233 and 415 K, UV absorption cross sections of CCl_3CHO and their temperature dependence, and quantum yields for production of H, O, and Cl atoms. Using these data and estimates of the heterogeneous loss of chloral, we have evaluated its atmospheric degradation pathways.

Experimental Section

The apparatuses used in this study were (1) a pulsed laser photolysis-laser-induced fluorescence (PLP-LIF) system to measure the rate coefficient for OH reaction with CCl_3CHO, (2) a diode array spectrometer to measure the UV absorption cross sections of CCl_3CHO as a function of temperature, (3) a pulsed laser photolysis-vacuum UV resonance fluorescence (PLP-RF) apparatus to measure the quantum yields for the production of atomic species (H, O, and Cl), and (4) a gas chromatograph to analyze end products following pulsed laser photolysis of CCl_3CHO. The apparatuses are described separately below.

OH Rate Coefficients. The apparatus and procedures employed to measure k_5 are described in detail elsewhere.[13,14] Therefore, only a brief summary is presented below.

A 150 cm^3 jacketed Pyrex reactor mounted in a vacuum housing was heated or cooled by circulating a fluid from a thermostated bath through its jacket. Gas mixtures containing the OH precursor, buffer gas, and chloral were flowed slowly through the cell (linear flow velocity 5−15 cm s^{-1}). The concentration of chloral in the flowing gas mixture was measured by its absorption at 213.9 nm (Zn pen-ray lamp) in two 100 cm long cells, one located before and the other after the reactor. The measured concentrations were the same, to within 2%, showing that there was no significant loss of chloral in the reactor.

The OH radicals were produced as follows: (1) photolysis of H_2O_2 at 248 nm (KrF excimer laser, laser fluence 3−15 mJ cm^{-2} pulse^{-1}), (2) photolysis of O_3/H_2O at 266 nm (fourth harmonic of Nd:YAG laser, laser fluence 1−3 mJ cm^{-2} pulse^{-1}), and (3) photolysis of HONO at 355 nm (third harmonic of Nd:YAG laser, laser fluence 8−46 mJ cm^{-2} pulse^{-1}). The use of different OH sources enabled us to identify the possible influence of secondary reactions and thus reduce systematic errors.

All experiments were carried out under pseudo-first-order conditions in [OH] ($[CCl_3CHO]/[OH]_0 > 10^3$). Therefore, OH temporal profiles should follow a simple exponential rate law:

$$[OH]_t = [OH]_0 \exp(-k_5^I t) \qquad \text{(I)}$$

where $k_5^I = k_5[CCl_3CHO] + k_d$. k_d is the first-order rate coefficient for the loss of OH in the absence of CCl_3CHO and is due to the reaction of OH with its photolytic precursors (and impurities in the precursor, e.g., NO_2 in HONO), diffusion out of the detection zone and reaction with impurities in the bath gas. The values of k_5 were obtained from the slopes of plots of k_5^I vs $[CCl_3CHO]$. Most of the experiments were performed at a total pressure of around 100 Torr of either He or a mixture of He and SF_6. However, 24 Torr of He was used in one experiment at room temperature to check for the pressure dependence of k_5.

UV Absorption Cross Sections. UV absorption cross sections of CCl_3CHO were measured over the wavelength range 200−345 nm at seven temperatures between 240 and 360 K. A D_2 lamp (30 W) coupled to a 0.25 m spectrometer equipped with a diode array detector was used. The spectrometer covered a 80 nm block with a resolution of 1 nm. The absorption spectrum between 200 and 345 nm was obtained from measurements in two overlapping wavelength blocks of 80 nm width. To minimize any systematic error in measuring the temperature dependence of CCl_3CHO cross sections, we used two absorption cells (35 cm long) connected to each other and filled with the same CCl_3CHO sample;[13,15] one cell was at 298 ± 2 K and the other at a variable temperature. Thermostated liquid was circulated through the jacket of the second cell to regulate its temperature. We measured the ratios of the absorbances in the two cells at various CCl_3CHO pressures. The measured relative temperature dependence of the cross sections were placed on an absolute scale by measuring the absorption cross sections at room temperature (298 K).

The UV absorption cross section of CCl_3CHO at 213.9 nm used in the OH kinetic measurements, $(3.26 \pm 0.12) \times 10^{-19}$ cm^2 molecule^{-1}, was determined by slowly flowing the compound through a 25.4 cm or a 10 cm long absorption cell at a known pressure and measuring the absorbance. The quoted error is 2σ precision of the mean of many sets of measurements. This value agrees very well with the one measured using the diode array spectrometer, $(3.18 \pm 0.10) \times 10^{-19}$ cm^2 molecule^{-1} (see below), as well as those reported by Gillotay et al.[11] (3.5×10^{-19} cm^2 molecule^{-1} at 295 K) and by Rattigan et al.[2] (3.1×10^{-19} cm^2 molecule^{-1} at 296 K).

Photolysis Quantum Yields. CCl_3CHO was flowed slowly through a reactor (flow velocity = 15−20 cm s^{-1}) and photolyzed at 193 (ArF), 248 (KrF), or 308 (XeCl) nm, using pulsed excimer lasers. H, O, and Cl atoms produced upon photolysis were detected using atomic resonance fluorescence.

* Address correspondence to this author. E-mail: talukdar@al.noaa.gov. NOAA, R/AL2, 325 Broadway, Boulder, CO 80305.
† National Oceanic and Atmospheric Administration.
‡ CIRES, University of Colorado.
§ CNRS-LCSR.
|| Also associated with the Department of Chemistry and Biochemistry, University of Colorado, Boulder, Colorado 80309.

TABLE 1: Summary of Experimental Conditions and Measured Values of k_5

T (K)	OH source[a]	$[OH]_0$ (10^{10} molecule cm^{-3})[b]	buffer gas[c]/ pressure (Torr)	$[CCl_3CHO]$ (10^{15} molecule cm^{-3})	$k_5 \pm \sigma$ (10^{-13} cm^3 molecule^{-1} s^{-1})[d]
233	HONO	11	He/SF_6/50	1.3−12	6.69 ± 0.09
233	HONO	43	He/SF_6/104	1.8−13.9	7.01 ± 0.10
251	O_3/H_2O	6−20	He/100	1.1−11.6	7.05 ± 0.09
252	HONO	21	He/SF_6/105	1.2−13.1	7.55 ± 0.06
253	HONO	40	He/SF_6/104	1.5−12.8	7.94 ± 0.02
271	HONO	46	He/SF_6/104	1.2−11.6	7.62 ± 0.04
295	HONO	38	He/SF_6/106	1.2−13.8	7.98 ± 0.06
295	HONO	37	He/24	1.4−13.8	7.88 ± 0.05
296	H_2O_2	25	He/105	1.9−21.6	7.47 ± 0.34
297	O_3/H_2O	5−20	He/103	1.7−16.3	8.04 ± 0.15
323	HONO	48	He/105	0.9−13.1	8.33 ± 0.05
327	H_2O_2	6−24	He/105	1.8−19.0	9.20 ± 0.12
348	O_3/H_2O	4−16	He/105	1.5−15.5	8.85 ± 0.13
374	H_2O_2	4−16	He/105	1.2−15.5	10.6 ± 0.61
413	O_3/H_2O	5−15	He/105	1.4−11.4	10.2 ± 0.27
415	H_2O_2	4−18	He/104	1.4−11.7	11.7 ± 0.08

[a] Photolysis wavelengths are 355 nm for HONO, 266 nm for O_3/H_2O, and 248 nm for H_2O_2. [b] $[OH]_0$ was calculated using the measured laser power and precursor concentration. [c] SF_6 was ~40% of the total pressure. [d] Uncertainties are the 1σ precision of the least-squares fits of k_5^I vs $[CCl_3CHO]$.

Detection of these atoms, acquisition of the temporal profiles, processing of the data, and determination of quantum yields by using a reference compound are discussed in detail elsewhere.[14,16,17]

All quantum yields were measured at room temperature, 298 ± 2 K. The photolysis laser fluence was varied by a factor of 2 and the chloral concentration was varied by a factor of 10. The H atom quantum yield was measured at 193, 248, and 308 nm. At 193 nm, photolysis of HBr was used as the reference. Photolysis of CH_3SH at 248 nm was employed as the reference to determine the H atom yield at both 248 and 308 nm. Photolysis of O_3 was used as the reference to determine the O atom, O(^{3}P), yields at both 248 and 308 nm. Since photolysis of O_3 predominantly generates O(^{1}D), O atom yields were measured in 1:1 mixtures of He:N_2 at total pressures in the range 50−100 Torr. N_2 in the mixture completely quenched O(^{1}D) to O(^{3}P) within 1 μs. The Cl atom quantum yield was measured only at 308 nm and Cl_2 was used as the reference compound.

The photolyte concentration was measured by UV absorption in a 100 cm long glass cell equipped with quartz windows and located upstream of the photolysis cell. The O_3 concentration was measured by absorption at 253.7 nm. Concentrations of both HBr and chloral were measured using 184.9 nm (Hg pen ray lamp), while that of CH_3SH was measured using 213.9 nm (Zn lamp). In addition to UV absorption, the concentration of chloral was also measured using calibrated mass flow meters. The detection sensitivity for H, O, and Cl atoms in the reactor via resonance fluorescence was determined to be 2×10^8, 1×10^9, and 1×10^9 atom cm^{-3}, respectively,[16] for 1 s integration under the conditions of our measurements.

Materials. The bath gases used had the following purity: He >99.9995% (UHP), SF_6 >99.99% (Instrument grade), and O_2 >99.999% (UHP). Helium was bubbled through the H_2O_2 sample for several days prior to use to reduce the water concentration. The H_2O_2 purity was estimated to be >90%. CCl_3CHO, devoid of inhibitors, was purified by trap-to-trap distillation with collection of the middle fraction. The manufacturer stated purity was 99.6%. According to the supplier (Crescent Chemicals CO.), the sample contained traces of 2,2-dichloroethanol, 2,2,3 trichlorobutanol, water, and HCl. Gas chromatographic analysis using a DB-5 column and a flame ionization detector (FID) showed a few peaks due to these impurities. Assuming that the response of the flame ionization detector for these impurities is the same as that for CCl_3CHO, we estimate that the detected impurities constituted <0.4% of chloral. Therefore, we assume that the purified sample of CCl_3CHO had a purity >99.6%.

Results and Discussion

OH Rate Coefficients. As mentioned in the Experimental Section, OH temporal profiles were measured in an excess of chloral. The second-order rate coefficient k_5 was derived from the linear least-squares fit of the measured values of k_5^I at various $[CCl_3CHO]$ to the expression, $k_5^I = k_5[CCl_3CHO] + k_d$. The obtained values of k_5 are listed in Table 1 along with the experimental conditions used to derive these rate constants. In general, the precision of these measurements, as indicated by the slope of the k_5^I vs $[CCl_3CHO]$ plots were within 5% at the 2σ level.

At room temperature (nominally 295−297 K in the present study) we measured k_5 using three different sources of OH. We also varied pressures from 24 to 100 Torr of He (in one case we used a mixture of 60 Torr of He and 50 Torr of SF_6) and $[OH]_0$ from 5 to 40×10^{10} cm^{-3}. In all cases, the OH temporal profiles were exponential and the plots of k_5^I vs $[CCl_3CHO]$ were linear. The obtained values of k_5 did not vary, within the precision of our measurements, with the experimental conditions. The intercept obtained by the linear least-squares analysis of k_5^I vs $[CCl_3CHO]$ data agreed with the measured value of k_d, which was measured by following the temporal profile of OH in the absence of chloral. Therefore, we believe that the measured values of k_5 at room temperature were not affected by secondary reactions. The four values of k_5 measured between 295 and 297 K were normalized to 298 K using an E/R value of 240 K (see below) and a weighted average of this value was used to derive k_5(298 K). We estimate an uncertainty in the measurement of $[CCl_3CHO]$ of about 7% (at 95% confidence level) and this is added to the standard deviation of the mean of the weighted average to obtain the uncertainty in the average value of k_5(298 K) given in Table 2.

Use of the O_3/H_2O mixture always led to the expected exponential OH decays and invariance of measured k_5 on experimental variables such as $[OH]_0$, laser fluence, pressure, and linear gas flow rate through the reactor. Similarly, the variation of these parameters while using H_2O_2 or HONO, at the temperature shown in Table 1, had no effect on the measured rate constants. However, there were some difficulties with using

TABLE 2: Comparison of the Previous Values of k_5 with Our Results

k_1(298 K)[a] (10^{-13} cm^3 molecule^{-1} s^{-1})	A (10^{-12} cm^3 molecule^{-1} s^{-1})	$f(298)$[b]	$(E/R \pm \Delta E/R)$ (K)	temp (K)	measurement technique[c]	ref
15.6 ± 3.3	(12 ± 3)	1.2	600 ± 100	298−520	DF-RF	4
17.8 ± 3.1				298	RR[d], PR-RA	5
8.6 ± 1.7				298	PLP-RF	3
16 ± 2				298	RR[e], PLP-RF, PLP-RA	6
10.5 ± 1.8				298	RR[f]	1
12.8 ± 2.5				298	DF-RF	1
8.9 ± 1.5				298	DF-EPR	1
8.3 ± 0.8[g]	1.79[h]	1.1	240 ± 60	233−415	PLP-LIF	this work

[a] 2σ uncertainties as quoted in the references. The quoted uncertainty for this work includes estimated systematic errors. [b] The uncertainty at a given temperature is given by $f(T) = f(298) \exp |[(\Delta E/R)((1/298) - (1/T))]|$. [c] DF, discharge flow; RF, resonance fluorescence; RR, relative rate; PR, pulsed radiolysis; RA, resonance absorption; PLP, pulsed laser photolysis; EPR, electron paramagnetic resonance; LIF, laser-induced fluorescence. [d] $CH_3COOC_2H_5$ with ($k_{OH} = 1.75 \times 10^{-12}$ cm^3 molecule^{-1} s^{-1}) was used as the reference compound. [e] $C_6H_5CH_3$ ($k_{OH} = 5.96 \times 10^{-12}$ cm^3 molecule^{-1} s^{-1}) was used as the reference compound. [f] Isobutane ($k_{OH} = 2.34 \times 10^{-12}$ cm^3 molecule^{-1} s^{-1}) was used as the reference compound. [g] k_{298K} obtained from the weighted average of our values around room temperature after correction for the difference in T. The quoted error is the sum of the precision and the estimated systematic error in measuring [CCl_3CHO] at 95% confidence level. [h] "A" has been adjusted to reproduce k_{298K}.

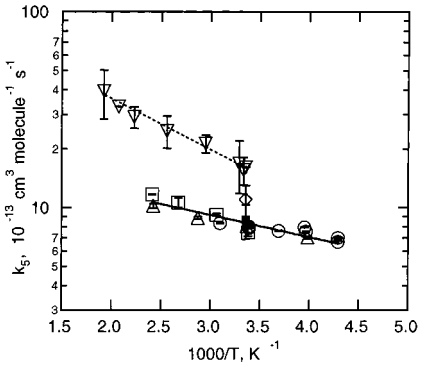

Figure 1. Plot of k_5 (on a logarithmic scale) vs $1/T$ from this work and previous work. Our data: open circles (HONO photolysis), open squares (H_2O_2 photolysis), open triangles (O_3 photolysis). The solid line is the weighted linear least-squares fit of our data to the Arrhenius expression to get $k_5(T) = 1.86 \times 10^{-12} e^{-240/T}$ cm^3 molecule^{-1} s^{-1}. Results from previous kinetic studies are plotted for comparison as Dóbé et al.[4] (open inverted triangle and dotted line), Balestra et al.[3] (solid square), and Barry et al.[1] (open diamond).

HONO at $T > 350$ K and using H_2O_2 at $T < 270$ K as the OH precursors. In these cases, OH temporal profiles were not strictly exponential and yielded progressively lower values of k_5^I at longer reaction times. The k_5 values obtained from fitting only the initial portions of the temporal profiles to eq I yielded values that were 10−20% lower than those measured using O_3/H_2O mixtures as the OH precursor. It should be noted that the values of k_5 measured using O_3/H_2O at $T > 350$ K and $T < 270$ K, where the OH temporal profiles were exponential, agreed with the values obtained by extrapolating the data derived from HONO or H_2O_2 source at $T < 350$ K or $T > 270$ K, respectively. We suspect that chloral may have undergone reaction with H_2O_2 on the walls and led to a product that regenerated OH on a longer time scale. We do not know what caused the nonexponential OH temporal profiles when using HONO as the OH source at $T > 350$ K. Therefore, we discarded the values of k_5 measured using H_2O_2 at $T < 270$ K and HONO at $T > 350$ K.

The measured values of k_5 shown in Table 1 are plotted in the Arrhenius form in Figure 1. They were fitted to the conventional Arrhenius form,

$$k = Ae^{-E/RT} \qquad \text{(II)}$$

The obtained values of A and E/R are listed in Table 2 along with our k_5(298 K) value and those reported in previous studies.

Dóbé et al.[4] used the discharge flow-resonance fluorescence technique to measure k_5 between 298 and 520 K. At 298 K, the authors reported $k_5 = (1.56 \pm 0.33) \times 10^{-12}$ cm^3 molecule^{-1} s^{-1}. This value is nearly a factor of 2 larger than ours and does not overlap even when the large reported uncertainty is included. It is of interest to note that Dóbé et al., using the same experimental setup, reported rate coefficients for the reactions of OH with $(CH_3)_2CHCHO$ (4.46×10^{-11} cm^3 molecule^{-1} s^{-1}) and $(CH_3)_3CCHO$ (5.16×10^{-11} cm^3 molecule^{-1} s^{-1}) that are higher than the current recommendations (2.63×10^{-11} and 2.65×10^{-11} cm^3 molecule^{-1} s^{-1}, respectively).[18] The higher values for these two reactions could be an indication of systematic errors in Dóbé et al.'s system.

The other previous measurements of k_5 were performed only at room temperature. Using the laser photolysis-resonance fluorescence method and the photolysis of nitric acid at 248 nm as the OH source, Balestra-Garcia et al.[3] obtained $k_5 = (0.86 \pm 0.17) \times 10^{-12}$ cm^3 molecule^{-1} s^{-1}, which is in good agreement with our value. The k_5 values of Nelson et al.,[5] and of Scollard et al.,[6] which are twice our values, are assumed to be superseded by the results of Barry et al.[1] at 298 K who obtained a rate constant that is about 30% higher than our value. As mentioned by Barry et al.,[1] secondary reactions led to faster loss of chloral in the relative rate measurements of Nelson et al.[5] and Scollard et al.[6] These two relative rate determinations were made in the same laboratories, using the photolysis of CH_3-ONO in air for the OH source. In their papers,[5,6] the authors indicated that the reactions of OH with chlorinated aldehydes in the presence of O_2 lead to a chain reaction involving chlorine atoms. Barry et al. suggested that even with added NO or C_2H_6 to scavenge Cl atoms, it is possible that not all Cl atoms were scavenged and loss of CCl_3CHO and the reference compounds, $C_6H_5CH_3$ and $CH_3C(O)OC_2H_5$, may have occurred. The rate coefficients for Cl atom reactions with $C_6H_5CH_3$ (5.9×10^{-11} cm^3 molecule^{-1} s^{-1})[19] and $CH_3COOC_2H_5$ (2×10^{-11} cm^3 molecule^{-1} s^{-1})[20] are larger than that of Cl with CCl_3CHO (5.4×10^{-12} cm^3 molecule^{-1} s^{-1}, this work). Therefore, one would expect Nelson et al. and Scollard et al. to measure a lower value of k_5 if Cl atoms were involved. Thus, the explanation of Barry et al. for the higher value of k_5 measured previously[5,6] is puzzling. Since the reference compounds are not photolyzed in this system, photolysis of chloral in these studies could lead to higher values for its loss rate and, hence, a higher measured value of k_5. Scollard et al. reported that variations in photolysis light intensity, which would alter the Cl atom production rate and CCl_3CHO loss rate, did not alter the measured value of k_5.

Barry et al.[1] used three different techniques to measure k_5. In the relative rate method, they produced OH by photolysis of O_3 in the presence of water vapor and used 2-methylpropane

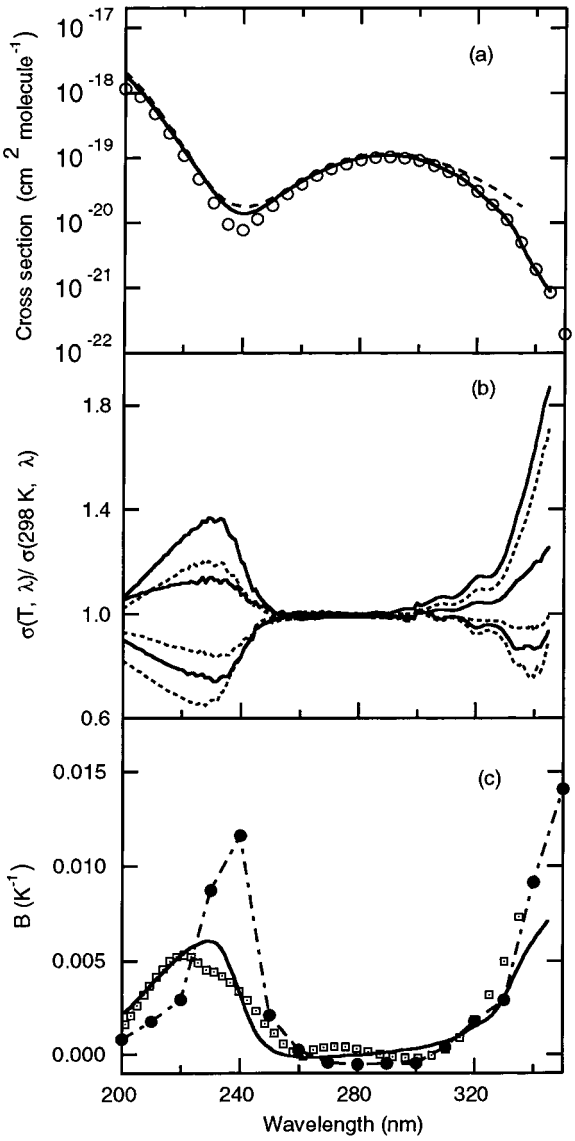

Figure 2. (a) Absorption cross section of CCl_3CHO (chloral) at 298 K measured in this work (solid line) as a function of wavelength. Data of Gillotay et al.[11] (dashed line) and Rattigan et al.[2] (open circles) are shown for comparison. (b) The ratio of absorption cross sections at temperatures T (360, 340, 320, 280, 260, and 240 K) to that at 298 K as a function of wavelength. Clearly, this ratio shows a decrease as temperature decreases except between 250 and 300 nm. The curves are in ascending order of temperatures, from 240 to 360 K as clearly seen around 230 and 340 nm. (c) Plot of the derived values of the B parameter that describes the temperature dependence of the absorption cross sections by the expression, $\ln[\sigma(T,\lambda)/\sigma(298,\lambda)] = B(T - 298)$, as a function of λ. Our results are shown as the solid line. The parametrization of the data from Gillotay et al.[11] (open squares) and Rattigan et al.[2] (solid circles) are shown for comparison.

as the reference compound ($k(OH + (CH_3)_3CH) = 2.34 \times 10^{-12}$ cm^3 molecule^{-1} s^{-1}). They obtained $k_5 = (1.05 \pm 0.18) \times 10^{-12}$ cm^3 molecule^{-1} s^{-1}. Using the discharge flow-resonance fluorescence and discharge flow-electron paramagnetic resonance methods, they obtained $(1.28 \pm 0.25) \times 10^{-12}$ and $(0.89 \pm 0.15) \times 10^{-12}$ cm^3 molecule^{-1} s^{-1}, respectively. Since these results overlapped within the quoted uncertainties, these authors reported a mean value of $(1.1 \pm 0.2) \times 10^{-12}$ cm^3 molecule^{-1} s^{-1} at 298 K. They did not attempt to identify the reasons for the small differences between the three methods. We note here that the values they obtained using the relative rate method and discharge flow-EPR technique agree quite well with our values.

Only Dóbé et al.[4] measured k_5 as a function of temperature. They measured k_5 between 298 and 520 K (see Figure 1) and reported a significantly larger activation energy than that measured by us. Since their 298 K value is also much larger than ours, as well as those from other previous studies, it is possible that Dóbé et al. had some systematic error in their measurements. If we were to assume that this systematic error was solely due to their quantification of chloral concentration, we could compare the measured values of activation energies. Clearly, Dóbé et al. reported a higher value of the activation energy than what we measured. It is not clear as to why this difference exists. It is possible that the Arrhenius plot for this reaction is curved. However, it is not clear that the Arrhenius plot can be nonlinear enough to account for the differences between the E/R values of Dóbé et al. and ours.

One of the potential sources of error in our measurements of k_5 is the presence of impurities in the sample of chloral. For the reasons listed below, we do not believe that the contributions of the impurities were significant. First, we used an uninhibited sample of chloral, which (according to the vendor) was >99.6% pure. Thus, the main possible source of olefins in chloral was avoided. Second, according to the vendor, possible impurities in chloral are 2,2-dichloroethanol, 2,2,3-trichlorobutanol, and HCl. We distilled this sample to drive off HCl and to purify it with respect to other impurities, and used only the middle fraction of the distillate. Third, we analyzed this middle fraction via GC analysis using a DB-5 column and a flame ionization detector (FID). This GC analysis showed a few peaks, which were very small compared to that of chloral. If we assume the FID response factor of the impurity peaks to be the same as that for chloral, we estimate that the mole fraction of the sum of these detected impurities to be less than 0.4% in the sample. Using this level of impurities, assuming the impurities to be chlorinated alcohols, and assuming a rate coefficient of $\sim 5 \times 10^{-12}$ cm^3 molecule^{-1} s^{-1} for their reaction with OH, we calculate their contribution to the measured value of k_5 to be less than 2%. (The rate coefficients for the reaction of OH with ethanol and butanol are 3.3×10^{-12} and 8.6×10^{-12} cm^3 molecule^{-1} s^{-1}, respectively. We do not expect the chlorination of these alcohols to increase their reactivity with OH.) Note that HCl, even if it were present, cannot contribute significantly to the measured value of k_5 because the rate coefficient for its reaction with OH is comparable to k_5. Because of these reasons, we are confident that reactive impurities did not contribute significantly to the measured values of k_5. This conclusion is supported by the Arrhenius behavior of k_5. If there were highly reactive impurities in chloral, we would expect k_5 to show a markedly curved Arrhenius line, with the lower temperature values being less sensitive to temperature. Last, it should be noted that the presence of the reactive impurities in our sample could not be the source of the discrepancy with the previous results because our measured values of k_5 are lower than those reported previously.

UV Absorption Cross Sections. The absorption cross sections for CCl_3CHO at 298 K measured in this work are plotted in Figure 2a and listed in Table 3 at 2 nm intervals. The temperature dependence of the CCl_3CHO cross sections is best visualized as the ratio $\sigma(T,\lambda)/\sigma(298K,\lambda)$, which is shown in Figure 2b. The absorption cross sections were measured at 360, 340, 320, 280, 260, and 240 K, and they all clearly decrease with decreasing temperature above 290 nm, the wavelengths important for atmospheric photolysis. The absorption cross sections also decrease with decreasing temperature below 240 nm.

TABLE 3: CCl_3CHO Absorption Cross Sections and Temperature Coefficients Defined by $\ln[\sigma(T,\lambda)/\sigma(298,\lambda)] = B(T - 298)$

λ (nm)	σ(298 K) (10^{-20} cm^2 molecule^{-1})	B (10^{-4} K^{-1})	λ (nm)	σ(298 K) (10^{-20} cm^2 molecule^{-1})	B (10^{-4} K^{-1})
200	186.9	22.0	274	8.46	−0.931
202	152.5	23.9	276	8.99	−0.584
204	121.8	27.2	278	9.49	−0.412
206	95.7	30.6	280	9.94	−0.481
208	73.8	34.1	282	10.3	−0.235
210	56.3	37.5	284	10.6	0.242
212	42.6	40.9	286	10.8	0.475
214	31.8	44.0	288	10.9	0.750
216	23.8	47.2	290	10.9	1.09
218	17.7	50.2	292	10.8	1.51
220	13.1	52.9	294	10.6	1.96
222	9.75	55.6	296	10.3	2.38
224	7.24	57.6	298	9.92	2.71
226	5.39	59.0	300	9.25	3.07
228	4.06	60.4	302	8.77	3.60
230	3.07	60.5	304	8.17	4.37
232	2.39	59.5	306	7.50	5.25
234	1.90	55.9	308	6.86	6.10
236	1.62	49.2	310	6.18	6.91
238	1.43	41.6	312	5.58	7.90
240	1.39	33.0	314	4.98	9.30
242	1.41	24.0	316	4.33	11.2
244	1.53	16.4	318	3.68	13.2
246	1.66	10.4	320	3.09	15.1
248	1.91	6.50	322	2.51	16.7
250	2.18	3.73	324	2.09	18.5
252	2.54	1.50	326	1.76	21.1
254	2.92	0.324	328	1.43	25.0
256	3.36	−0.569	330	1.12	30.3
258	3.84	−0.877	332	0.849	36.6
260	4.35	−1.23	334	0.590	43.3
262	4.90	−1.65	336	0.373	49.8
264	5.48	−1.62	338	0.261	55.6
266	6.07	−1.50	340	0.188	60.2
268	6.68	−1.41	342	0.136	65.0
270	7.28	−1.22	344	0.100	69.0
272	7.88	−1.07			

The measured temperature-dependent absorption cross section data is well represented by the following parametrization:

$$\ln \frac{\sigma(T,\lambda)}{\sigma(298,\lambda)} = B(T - 298) \qquad \text{(III)}$$

The B parameter values obtained from the least-squares fit to the data are listed in Table 3 along with the room-temperature cross section. The parametrization reproduces the measured absorption cross sections to within ±1% up to 300 nm, and to within ±5% above 300 nm. The derived B values are also plotted in Figure 2c.

The absorption cross section data from the studies of Gillotay et al.[11] and Rattigan et al.[2] are also plotted in Figure 2a for comparison. The agreement between the three studies, in general, is good. Our data are in very good agreement with that of Rattigan et al. at $\lambda > 290$ nm, the region of atmospheric photolysis. However, the agreement with the Gillotay et al. data in this wavelength region is not as good. The source of the differences with the Gillotay et al. data is not known.

Gillotay et al.[11] and Rattigan et al.[2] also reported the temperature dependence of the CCl_3CHO absorption cross sections. The B parameters obtained from their cross sections are shown in Figure 2c for comparison. Although there are significant differences at the short wavelengths, the derived B parameters are in good agreement in the wavelength range of atmospheric interest.

Photolysis Quantum Yields for Atoms. The concentration of X (X = H, O, or Cl) produced in the pulsed photolysis of CCl_3CHO is given by

$$[X] = [CCl_3CHO]\, \sigma_\lambda(CCl_3CHO)\, \Phi_\lambda^X(CCl_3CHO)\, F(\lambda) \qquad \text{(IV)}$$

where $F(\lambda)$ is the photolysis laser fluence (photon cm^{-2} pulse^{-1}) at wavelength λ, $\sigma_\lambda(CCl_3CHO)$ is the absorption cross section of chloral (cm^2 molecule^{-1}), and $\Phi_\lambda^X(CCl_3CHO)$ is the quantum yield for production of X in the photolysis of chloral at wavelength λ. The atomic resonance fluorescence signal, $S(X)$, is proportional to the atom concentration, i.e., $S(X) = C[X]$, where C is a constant. Therefore,

$$S(X) = C[CCl_3CHO]\, \sigma_\lambda(CCl_3CHO)\, \Phi_\lambda^X(CCl_3CHO)\, F(\lambda) \qquad \text{(V)}$$

Similarly, the signal obtained upon photolyzing the reference compound, Ref, is

$$S(X)_{Ref} = C[X]_{Ref} = C[Ref]\, \sigma_\lambda(Ref)\, \Phi_\lambda^X(Ref)\, F(\lambda) \qquad \text{(VI)}$$

In these experiments, the laser fluence, $F(\lambda)$, was monitored with a power meter after the reaction cell. We plotted $S(X)_{Ref}/F(\lambda)$ vs [Ref] to yield m_1 as the slope,

$$m_1 = C\sigma_\lambda(Ref)\, \Phi_\lambda^X(Ref) \qquad \text{(VII)}$$

A similar plot for photolysis of CCl_3CHO yielded m_2 as the slope,

$$m_2 = C\sigma_\lambda(CCl_3CHO)\, \Phi_\lambda^X(CCl_3CHO) \qquad \text{(VIII)}$$

Assuming the coefficient C is the same for the reference and chloral experiments, eqs VII and VIII can be combined to yield the quantum yield, $\Phi_\lambda^X(CCl_3CHO)$, for the formation of X in chloral photolysis,

$$\Phi_\lambda^X(CCl_3CHO) = \Phi_\lambda^X(Ref)\frac{m_2}{m_1}\frac{\sigma_\lambda(Ref)}{\sigma_\lambda(CCl_3CHO)} \qquad \text{(IX)}$$

Therefore, the quantum yield in the photolysis of CCl_3CHO is determined relative to a reference compound from measured concentrations, measured atomic fluorescence signals, and the known quantum yield of the reference compound. The absolute values of the laser fluence are not required. The reference compounds used in this study are listed in the Experimental Section.

All quantum yields were measured at 298 K and are summarized in Table 4. The absorption cross sections for the various reference compounds used here are listed in Table 5. As shown in Table 4, the yields of O and H atoms were found to be small or below our detection limit at 193, 248, and 308 nm. It is not surprising that the quantum yield for O atom is essentially zero because there are no thermodynamically allowed channels for O atom production. As in the case of acetaldehyde,[21] our data clearly shows that H atoms are not produced with a significant yield in the band responsible for atmospheric photolysis.

The quantum yield for the production of Cl atoms in the 308 nm photolysis (laser fluence = 2−30 mJ cm^{-2}) of chloral was measured by photolyzing (2.6−15) × 10^{13} cm^{-3} of chloral in 45−55 Torr of He. The temporal profiles of Cl atoms were measured and the initial concentrations of Cl atoms were obtained by extrapolating the temporal profiles to time zero. Clearly, Cl atoms were observed upon chloral photolysis. The yield of chlorine atoms was determined as described above to be 1.3 ± 0.3. The quoted error includes the estimated uncertain-

TABLE 4: Summary of the Quantum Yields Determined in This Work

photolysis wavelength, nm	$\Phi(O^3P)$	$\Phi(H)$	$\Phi(Cl)$
193		0.04 ± 0.005	
248	<0.02	<0.01	
308	<0.01	<0.002	1.3 ± 0.3

TABLE 5: Absorption Cross Sections Used in the Data Analysis

molecule	λ (nm)	σ (10^{-18} cm^2 molecule^{-1})	reference
CCl_3CHO	184.95	4.8	11
	193	3.4	11
	213.9	0.326	this work
	248	0.0191	this work
	308	0.0686	this work
O_3	248	10.8	27
	253.65	11.7	27
	308	0.134	27
Cl_2	308	0.170	28
HBr	184.95	2.36	29
	193	1.80	29
CH_3SH	213.9	1.49	30
	248	0.30	31

ties in the absorption cross sections of chloral and Cl_2 (reference compound), and in the measured concentrations of chlorine and chloral.

The unit yield of chlorine in chloral photolysis was surprising since the major expected photolysis channel was to produce CCl_3 and CHO radicals.[22] However, we believe that Cl atoms are indeed the primary photolysis products because of the following reasons. The measured chlorine atom concentration at a given concentration of chloral varied linearly with laser fluence from 2 to 38 mJ cm^{-2}. Also, the measured initial Cl atom concentration at a fixed value of the photolysis fluence varied linearly with chloral concentration. Therefore, we do not believe that a multiphoton process was responsible for the production of Cl atoms. These observations also exclude the possibility of Cl atom production via the sequential photolysis of chloral producing CCl_3 followed by its photolysis at 308 nm. A calculation also shows that the sequential photolysis would not account for the observed Cl atoms even if the absorption cross section of CCl_3 radicals produced in the photolysis at 308 nm were 1×10^{-16} cm^2. (The peak absorption cross section of thermalized CCl_3 radicals at its absorption maxima, 211 ± 2 nm, is $(1.45 \pm 0.35) \times 10^{-17}$ cm^2, but it is conceivable that vibrationally excited CCl_3 absorbs at longer wavelengths.) Variation of the gas flow velocity through the reactor did not affect the measured Cl atom quantum yield, thereby confirming that accumulation of the photolysis products did not contribute to the observed Cl atoms. It is not possible to produce CCl_3 radicals that are sufficiently energetic to undergo further dissociation to give CCl_2 and Cl atoms:

$$CCl_3CHO \rightarrow CCl_2 + Cl + CHO$$
$$\Delta H_f^0(298\ \mathrm{K}) = 137.8\ \mathrm{kcal\ mol^{-1}},\ \lambda \leq 207.7\ \mathrm{nm} \quad (7)$$

Therefore, we believe that Cl atoms are primary photolysis products. Since, it is not energetically possible to eliminate more than one Cl atom in the photodissociation at 308 nm, we assume that the quantum yield for Cl atoms in chloral photolysis at 308 nm is unity.

In the course of the Cl atom quantum yield measurements, it was observed that the reaction,

$$Cl + CCl_3CHO \rightarrow \text{products} \quad (8)$$

was rapid. Analyses of the Cl atom signal temporal profiles at various concentrations of CCl_3CHO yielded a room-temperature rate coefficient for reaction 8 of $(5.4 \pm 0.7) \times 10^{-12}$ cm^3 molecule^{-1} s^{-1}. The quoted uncertainty includes the 2σ precision of the slope of $k_8^I = k_8[CCl_3CHO] + k_d$ vs $[CCl_3CHO]$ plot (where k_d is the first-order rate constant for the loss of Cl in the absence of CCl_3CHO) and an estimated 8% uncertainty in CCl_3CHO concentration. At very high photolysis laser fluence ($\sim$37 mJ cm^{-2}), when the initial Cl atom concentrations were $>5 \times 10^{11}$ atom cm^{-3}, the Cl atom temporal profiles were nonexponential. The nonexponential behavior was likely due to the contributions of Cl atom reaction with other radicals at short reaction times. However, at lower concentrations the Cl atom temporal profiles were exponential for at least two lifetimes. Only low Cl atom concentration data were included in the rate coefficient determination.

Our value of k_8 is somewhat lower than that reported by Scollard et al.[6] ($(7.1 \pm 0.5) \times 10^{-12}$ cm^3 molecule^{-1} s^{-1}), and Platz et al.[23] ($(6.0 \pm 1.3) \times 10^{-12}$ cm^3 molecule^{-1} s^{-1}). Both of these studies used relative rate technique techniques with $C_6H_5CH_3$ (5.59×10^{-11} cm^3 molecule^{-1} s^{-1}) and C_2H_5Cl (8.04×10^{-12} cm^3 molecule^{-1} s^{-1}) as the reference compounds. Uncertainties in the rate coefficients for the reference compounds may be responsible for the differences in the reported values for reaction 8.

Stable End Products. In a few experiments, either pure CCl_3CHO ($\sim$20 Torr) or a $\sim$2% mixture of CCl_3CHO in He or O_2 (total pressure between 900 and 1100 Torr in a static cell) was photolyzed by many pulses (3000−60000 shots) from a KrF (248 nm) pulsed excimer laser in a 30 cm long cell. Most of the experiments were performed with low laser fluences, $\sim$1 mJ cm^{-2} pulse^{-1}, but fluences as high as 20 mJ cm^{-2} pulse^{-1} were used in a few cases. The postphotolysis mixture was analyzed using a gas chromatograph equipped with a flame ionization detector (FID) and a thermal conductivity detector (TCD).

We detected CO, $CHCl_3$, and C_2Cl_6 as products when CCl_3CHO neat (or in He) was photolyzed. Photolysis of CCl_3CHO/O_2 mixtures led to the formation of CO and $COCl_2$ and no $CHCl_3$ was observed. We did not deduce quantitative yields from these measurements. All the products, except phosgene, were identified by comparison with analytical standards. Phosgene was identified on the basis of the retention time for the column used in our experiment. Calculations showed that the number of chloral molecules that absorbed light, and hence the number that dissociated, was much smaller than the number of chloral molecules destroyed. Therefore, it is clear that chloral was lost via a chain reaction mechanism. The absence of $CHCl_3$ in the presence of O_2, when CCl_3 radicals can be scavenged, shows that $CHCl_3$ is not a primary product of CCl_3CHO photolysis. Thus, the molecular channel in the photolysis of this aldehyde,

$$CCl_3CHO + h\nu \rightarrow CCl_3H + CO \quad (9)$$

does not appear to be important at 248 nm. Such a molecular channel is well established in the photolysis of H_2CO. Our observed products in the presence and absence of O_2 are consistent with the conclusion of Ohta and Mizoguchi[22] that the photodegradation of CCl_3CHO (wavelength range: 300−400 nm) in the presence of O_2 proceeds via a chain mechanism leading to CCl_2O, CO, and CO_2. On the basis of their observation, Ohta and Mizoguchi[22] speculated that the photodissociation of CCl_3CHO led to CCl_3 and HCO radicals that could propagate the chain reaction. Their speculation can be justified as follows: The absorption spectrum of chloral is

similar to that of other aldehydes with an absorption band centered around 300 nm. This band has been assigned to an n → p* electronic transition on the carbonyl group.[2] Atmospheric photolysis of CCl_3CHO takes place by absorption in this band. Thus, the primary photolysis products are expected to be CCl_3 and HCO radicals. Contrary to their interpretation, we believe that Cl atoms are the primary products in their photolysis experiments (wavelength range: 300−400 nm), as observed by us at 308 nm photolysis, and the following reactions of Cl and CCl_3CHO can lead to the products observed by both us and Ohta and Mizoguchi:

$$CCl_3CHO + h\nu \rightarrow CCl_2CHO + Cl \quad (6a)$$

$$CCl_3CHO + Cl \rightarrow CCl_3CO + HCl \quad (8)$$

$$CCl_3CO + M \rightarrow CCl_3 + CO + M \quad (10)$$

$$CCl_3 + O_2 + M \rightarrow CCl_3O_2 + M \quad (11)$$

$$2CCl_3O_2 \rightarrow 2CCl_3O + O_2 \quad (12)$$

$$CCl_3O + M \rightarrow COCl_2 + Cl + M \quad (13)$$

$$CCl_3CO + O_2 + M \rightarrow CCl_3COO_2 + M \quad (14)$$

$$2CCl_3COO_2 \rightarrow 2CCl_3CO_2 + O_2 \quad (15)$$

$$CCl_3CO_2 + M \rightarrow CCl_3 + CO_2 + M \quad (16)$$

If reaction 14 does not compete with reaction 13, one could still get CO_2 via Cl atom reaction with CO in the presence of O_2.

Atmospheric Lifetime of CCl_3CHO. The first-order rate coefficients for the tropospheric loss of CCl_3CHO due to its photolysis and reaction with OH were calculated using the methodology described earlier.[24] The diurnally averaged OH concentration profile and the solar flux for 30° N and July 4 with an overhead ozone column abundance of 305 DU for a US Standard Atmosphere[25] were those from our previous work.[24] The temperature-dependent absorption cross sections measured in this work were employed along with the standard temperature profile of the US Standard Atmosphere. The photodissociation quantum yield for removal of CCl_3CHO was taken to be unity on the basis of the Cl atom quantum yield from its photolysis at 308 nm, the center of the band, which leads to atmospheric photolysis. The calculated *J* value and the first-order rate coefficient for the loss via reaction with OH, are shown in Figure 3. The tropospheric photolysis lifetime is on the order of 5−10 h, while the lifetime via reaction with OH is 10−15 days.

In addition to the quantified loss due to OH reaction and photolysis, chloral may be removed from the troposphere via wet deposition and reactions with NO_3 or O_3. The reaction of chloral with ozone will be negligibly small because aldehydes do not react with ozone.[18] Even if we assume that NO_3 reacts with chloral with a rate coefficient of $\sim 2 \times 10^{-15}$ cm^3 molecule^{-1} s^{-1} at 298 K, the rate coefficient for the reaction of NO_3 with the analogous aldehyde, the lifetime of chloral with respect to this process would be ~1.5 year (assuming an average $[NO_3] \sim 1 \times 10^7$ cm^{-3}). Therefore, the contribution of NO_3 reaction to the removal of chloral is negligible. The Henry's law solubility constant for chloral in water is $\sim 3.4 \times 10^5$ M Atm^{-1}.[12] This value is similar to that of H_2O_2 in water. On the basis of the evaluated wet deposition removal rate for H_2O_2 of

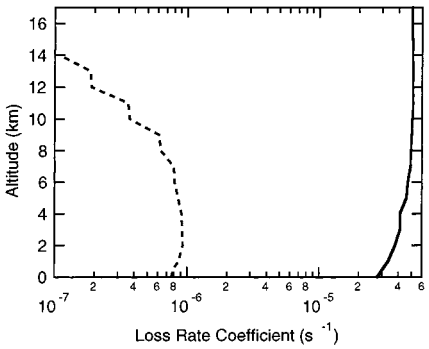

Figure 3. Calculated first-order rate coefficient for atmospheric loss of chloral as a function of altitude using diurnally averaged OH concentration profile, the solar flux for 30° N (summer), 305 DU of ozone, and a standard atmosphere temperature profile. The loss rate due to reaction with OH is given by the dashed line, while the loss rate via photolysis is shown as a solid line.

~5 days, we assume that chloral is removed by this process with a lifetime of 2−3 days. (Note: The H_2O_2 removal rate is not limited by its solubility, but rather by the frequency of precipitation). Thus, it is clear that the major loss process for chloral is photolysis, especially for that produced from CH_3CCl_3, which is destroyed mostly in the tropical mid-troposphere. It is possible that the lifetime of chloral, if emitted directly into the atmosphere, could be longer in the winter time and could be limited by nonphotolytic processes, such as wet deposition.

The tropospheric lifetime of CCl_3CHO is relatively short and is predominantly controlled by its photolysis. The photolysis of CCl_3CHO is expected to produce CCl_2O via the following sequence of reactions in the atmosphere

$$CCl_3CHO + h\nu \rightarrow CCl_2CHO + Cl \quad (6a)$$

$$CCl_2CHO + O_2 + M \rightarrow OOCCl_2CHO + M \quad (17)$$

$$OOCCl_2CHO + NO/(RO_2) \rightarrow OCCl_2CHO + NO_2/(RO + O_2) \quad (18)$$

$$OCCl_2CHO + M \rightarrow CCl_2O + HCO + M \quad (19)$$

The possible production of $CHCl_3$ via photolysis cannot be completely ruled out because we did not measure $CHCl_3$ yield in photolysis at longer wavelengths.

The reaction of chloral with OH also leads to the formation of CCl_2O in the troposphere via the following sequence of reactions:

$$OH + CCl_3CHO \rightarrow H_2O + CCl_3CO \quad (5)$$

$$CCl_3CO + O_2 + M \rightarrow CCl_3C(O)OO + M \quad (14)$$

$$CCl_3C(O)OO + NO/(RO_2) \rightarrow CCl_3C(O)O + NO_2/(RO + O_2) \quad (20)$$

$$CCl_3C(O)O + M \rightarrow CCl_3 + CO_2 + M \quad (16)$$

$$CCl_3 + O_2 + M \rightarrow CCl_3OO + M \quad (11)$$

$$CCl_3OO + NO\ (RO_2) \rightarrow CCl_3O + NO_2/(RO + O_2) \quad (21)$$

$$CCl_3O + M \rightarrow CCl_2O + Cl + M \quad (22)$$

Therefore, it appears that the degradation of chloral will lead to either CCl_2O or, to a small possible extent, $CHCl_3$.

The atmospheric fate of CCl_2O has been evaluated in a recent modeling study by Kindler et al.[26] They conclude that the tropospheric removal of CCl_2O is determined via wet deposition to be on the order of 70 days. We can estimate the lifetime of $CHCl_3$ to be ~0.5 year on the basis of the rate coefficient for its reaction with OH. Therefore, the chemical removal of CCl_3CHO in the troposphere leads to the production of significantly longer-lived species, CCl_2O and $CHCl_3$, and one cannot assume that destruction of methylchloroform and its main oxidation product, CCl_3CHO, completely prevents the transport of its chlorine to the stratosphere. Thus, stratospheric chlorine loading due to CH_3CCl_3 should include the transport of $COCl_2$ from the troposphere. This may also be important in analyzing the stratospheric $COCl_2$ abundance, which currently assumes that it originates only via stratospheric degradation of CH_3CCl_3. Finally, this production of longer-lived species in the atmospheric degradation of species points to a need for the complete understanding of such processes.

Acknowledgment. We thank J. L. Delfau and C. Vovelle for their help in gas chromatographic analysis. A.M. and G.L.B. thank the European Commission and CNRS (Direction des Relations Internationales) for support. This work was funded in part by NOAA's Climate and Global Change program.

References and Notes

(1) Barry, J.; Scollard, D. J.; Treacy, J. J.; Sidebottom, H. W.; Le Bras, G.; Poulet, G.; Teton, S.; Chichinin, A.; Canosa-Mas, C. E.; Kinnison, D. J.; Wayne, R. P.; Nielsen, O. J. *Chem. Phys. Lett.* **1994**, *221*, 353−358.

(2) Rattigan, O. V.; O.Wild; Jones, R. L.; Cox, R. A. *J. Photochem. Photobiol. A: Chem.* **1993**, *73*, 1−9.

(3) Balestra-Garcia, C.; LeBras, G.; MacLeod, H. *J. Phys. Chem.* **1992**, *96*, 3312−3316.

(4) Dóbé, S.; Khachatryan, L. A.; Berces, T. *Ber. Bunsen-Ges. Phys. Chem.* **1989**, *93*, 847−852.

(5) Nelson, L.; Shanahan, I.; Sidebottom, H. W.; Treacy, J.; Nielsen, O. J. *Int. J. Chem. Kinet.* **1990**, *22*, 577−590.

(6) Scollard, D. J.; Treacy, J. J.; Sidebottom, H. W.; Balestra-Garcia, C.; Laverdet, G.; LeBras, G.; Macleod, H.; Teton, S. *J. Phys. Chem.* **1993**, *97*, 4683−4688.

(7) DeMore, W. B.; Sander, S. P.; Golden, D. M.; Hampson, R. F.; Kurylo, M. J.; Howard, C. J.; Ravishankara, A. R.; Kolb, C. E.; Molina, M. J. Chemical Kinetics and Photochemical Data for Use in Stratospheric Modeling, Evaluation number 12. Jet Propulsion Laboratory, 1997.

(8) Rayez, M. T.; Scollard, D. J.; Treacy, J. J.; Sidebottom, H. W.; Balestra-Garcia, C.; Teton, S.; LeBras, G. *Chem. Phys. Lett.* **1994**, *223*, 452−458.

(9) Benson, S. W. *Thermochemical Kinetics*, 2nd ed.; Wiley: New York, 1976.

(10) Cohen, N.; Benson, S. W. *Chem. Rev.* **1993**, *93*, 2419−2438.

(11) Gillotay, D.; Simon, P. C.; Dierickx, L. Ultraviolet absorption cross-sections of some carbonyl compounds and their temperature dependence. Quadrennial ozone symposium; University of Viginia: Charlottesville, VA, 1992.

(12) Betterton, E. A.; Hoffmann, M. R. *Environ. Sci. Technol.* **1988**, *22*, 1415−1418.

(13) Talukdar, R. K.; Burkholder, J. B.; Schmoltner, A.-M.; Roberts, J. M.; Wilson, R.; Ravishankara, A. R. *J. Geophys. Res.* **1995**, *100*, 14163−14173.

(14) Vaghjiani, G. L.; Ravishankara, A. R. *J. Chem. Phys.* **1990**, *92*, 996−1003.

(15) Burkholder, J. B.; Talukdar, R. K.; Ravishankara, A. R.; Solomon, S. *J. Geophys. Res.* **1993**, *98*, 22937−22948.

(16) Talukdar, R. K.; Warren, R. F.; Vaghjiani, G. L.; Ravishankara, A. R. *Int. J. Chem. Kinet.* **1992**, *24*, 973−982.

(17) Warren, R. F.; Ravishankara, A. R. *Int. J. Chem. Kinet.* **1993**, *25*, 833−844.

(18) Atkinson, R. *J. Phys. Chem. Ref. Data* **1994**, Monograph No. 2.

(19) Shi, J.; Bernhard, M. J. *Int. J. Chem. Kinet.* **1997**, *29*, 349−358.

(20) Notario, A.; Bras, G. L.; Mellouki, A. *J. Phys. Chem. A* **1998**, *102*, 3112−3117.

(21) Atkinson, R.; Baulch, D. L.; Cox, R. A.; R. F. Hampson, J.; Kerr, J. A.; Troe, J. *J. Phys. Chem. Ref. Data* **1992**, *21*, 1125−1593.

(22) Ohta, T.; Mizoguchi, I. *Int. J. Chem. Kinet.* **1980**, *12*, 717−727.

(23) Platz, J.; Nielsen, O. J.; Sehsted, J.; Wallington, T. J. *J. Phys. Chem.* **1995**, *99*, 6570−6579.

(24) Talukdar, R. K.; Burkholder, J. B.; Hunter, M.; Gilles, M. K.; Roberts, J. M.; Ravishankara, A. R. *J. Chem. Soc., Faraday Trans.* **1997**, *93*, 2797−2805.

(25) U.S. Standard Atmosphere, 1976. NOAA/NASA/USAF, 1976.

(26) Kindler, T. P.; Chameidies, W. L.; Wine, P. H.; Cunnold, D. M.; Alyea, F. N.; Franklin, J. A. *J. Geophys. Res.* **1995**, *100*, 1235−1251.

(27) Molina, L. T.; Molina, M. J. *J. Geophys. Res.* **1986**, *91*, 14501−14508.

(28) Maric, D.; Burrows, J. P.; Meller, R.; Moortgat, G. K. *J. Photochem. Photobiol. A: Chemistry* **1993**, *70*, 205−214.

(29) Huebert, B. J.; Martin, R. M. *J. Phys. Chem.* **1968**, *72*, 3046−3048.

(30) Wine, P. H.; Thompson, R. J.; Semmes, D. H. *Int. J. Chem. Kinet.* **1984**, *16*, 1623−1636.

(31) Wine, P. H.; Nicovich, J. M.; Hynes, A. J.; Wells, J. R. *J. Phys. Chem.* **1986**, *90*, 4033−4037.